

Supporting Information

The effect of indium substitution on the structure and NLO property of $\text{Ba}_6\text{Cs}_2\text{Ga}_{10}\text{Se}_{20}\text{Cl}_4$

Yan-Yan Li^a, Peng-Fei Liu,^a Hua Lin,^a Mei-Tian Wang^b and Ling Chen*^a

^aKey Laboratory of Optoelectronic Materials Chemistry and Physics, Fujian Institute of Research on the Structure of Matter, Chinese Academy of Sciences, Fuzhou, Fujian 350002, People's Republic of China

^bSwiss Light Source, Paul Scherrer Institute, CH-5232 Villigen, Switzerland

To whom correspondence should be addressed. E-mail: chenl@fjirsm.ac.cn

Tel: (011) 86-591-63173131.

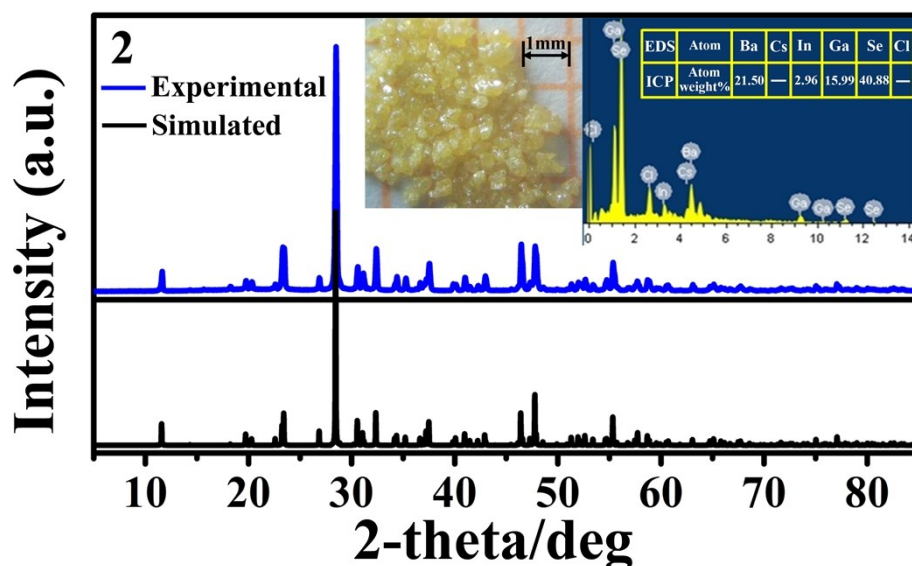


Figure S1. Experimental and calculated powder XRD of $\text{Ba}_6\text{Cs}_2\text{InGa}_{10}\text{Se}_{20}\text{Cl}_4$, **2** with inset of crystal photos, EDX and ICP results.

Table S1. The ICP data of $\text{Ba}_6\text{Cs}_2\text{In}_2\text{Ga}_8\text{Se}_{20}\text{Cl}_4$, **1** and $\text{Ba}_6\text{Cs}_2\text{InGa}_9\text{Se}_{20}\text{Cl}_4$, **2**.

Comp.	Element	Weight%	Formula
1 $\text{Ba}_6\text{Cs}_2\text{In}_2\text{Ga}_8\text{Se}_{20}\text{Cl}_4$	Ba	20.42	$\text{Ba}_{6.30}\text{In}_{2.0}\text{Ga}_{8.01}\text{Se}_{18.64}$
	In	5.42	
	Ga	13.18	
	Se	34.73	
2 $\text{Ba}_6\text{Cs}_2\text{InGa}_9\text{Se}_{20}\text{Cl}_4$	Ba	21.50	$\text{Ba}_{6.07}\text{In}_{1.0}\text{Ga}_{8.90}\text{Se}_{20.08}$
	In	2.96	
	Ga	15.99	
	Se	40.88	

Table S2. Crystallographic data and refinement details for $\text{Ba}_6\text{Cs}_2\text{In}_x\text{Ga}_{10-x}\text{Se}_{20}\text{Cl}_4$ ($x = 2, \mathbf{1}; x = 1, \mathbf{2}$) from different batches.

Comp.	1		2	
Formula	Cry#1	Cry#2	Cry#1	Cry#2
$\text{Ba}_6\text{Cs}_2\text{In}_{1.98}\text{Ga}_{8.02}\text{Se}_{20}\text{Cl}_4$	$\text{Ba}_6\text{Cs}_2\text{In}_{1.97}\text{Ga}_{8.03}\text{Se}_{20}\text{Cl}_4$	$\text{Ba}_6\text{Cs}_2\text{In}_{0.97}\text{Ga}_{9.03}\text{Se}_{20}\text{Cl}_4$	$\text{Ba}_6\text{Cs}_2\text{In}_{0.96}\text{Ga}_{9.04}\text{Se}_{20}\text{Cl}_4$	
fw	1798.68	1798.45	1775.90	1775.68
crystal system		Tetragonal		
crystal color		light yellow		
space		<i>I</i> -4 (no.82)		
$a=b(\text{\AA})$	8.7627(7)	8.7583(7)	8.7444(4)	8.7459(4)
$c (\text{\AA})$	15.817(3)	15.808(3)	15.732(2)	15.734(2)
$V (\text{\AA}^3)$	1214.5(3)	1212.6(3)	1202.9(2)	1203.5(2)
Z	2	2	2	2
D_c (g/cm^3)	4.919	4.926	4.903	4.900
$\mu (\text{mm}^{-1})$	26.748	26.791	27.086	27.074
GOOF on r_{c}	1.044	1.036	1.213	1.148
$R_1, wR_2 (I > 2\sigma(I))$ ^a	0.0294, 0.0642	0.0289, 0.0741	0.0211, 0.0428	0.0180, 0.0350
R_1, wR_2 (all data)	0.0323, 0.0649	0.0297, 0.0746	0.0294, 0.0819	0.0197, 0.0351
largest diff. Peak and hole(e/ \AA^3)	1.031, -0.909	1.115, -1.206	1.620, -2.225	0.563, -0.764
Absolute structure parameter	0.00(4)	0.00(3)	0.00(5)	0.00(2)

^a $R_1 = \Sigma ||F_o| - |F_c|| / \Sigma |F_o|$, $wR_2 = [\sum w(F_o^2 - F_c^2)^2 / \sum w(F_o^2)]^{1/2}$

Table S3. Atomic coordinates and equivalent isotropic displacement parameters of **1**, Ba₆Cs₂In₂Ga₈Se₂₀Cl₄.

1, Ba ₆ Cs ₂ In ₂ Ga ₈ Se ₂₀ Cl ₄						
Atom	Wyck.	x	y	z	U _{eq} (Å ²)	S.O.F
Ba	8g	0.26097(6)	0.37151(7)	0.36409(3)	0.0274(2)	0.75
Cs	8g	0.26097(6)	0.37151(7)	0.36409(3)	0.0274(2)	0.25
In1	2d	0.0000	0.5000	0.7500	0.0153(5)	0.52(2)
Ga1	2d	0.0000	0.5000	0.7500	0.0153(5)	0.48(2)
In2	8g	0.40115(9)	0.30879(9)	0.08426(5)	0.0143(3)	0.12(2)
Ga2	8g	0.40115(9)	0.30879(9)	0.08426(5)	0.0143(3)	0.88(2)
Se1	8g	0.2822(2)	0.1243(2)	0.17561(5)	0.0219(2)	1
Se2	8g	0.1867(2)	0.4139(2)	0.00726(6)	0.0225(2)	1
Se3	4e	0.0000	0.0000	0.32179(9)	0.0346(4)	1
Cl1	2c	0.0000	0.5000	0.2500	0.039(2)	1
Cl2	2a	0.0000	0.0000	0.0000	0.036(2)	1

Table S4. Atomic coordinates and equivalent isotropic displacement parameters of **2**, Ba₆Cs₂InGa₉Se₂₀Cl₄.

2, Ba ₆ Cs ₂ InGa ₉ Se ₂₀ Cl ₄						
Atom	Wyck.	x	y	z	U _{eq} (Å ²)	S.O.F
Ba	8g	0.2612(2)	0.3704(2)	0.36381(6)	0.0269(3)	0.75
Cs	8g	0.2612(2)	0.3704(2)	0.36381(6)	0.0269(3)	0.25
In1	2d	0.0000	0.5000	0.7500	0.0136(8)	0.28(2)
Ga1	2d	0.0000	0.5000	0.7500	0.0136(8)	0.72(2)
In2	8g	0.4028(2)	0.3090(2)	0.08456(9)	0.0132(5)	0.05(2)
Ga2	8g	0.4028(2)	0.3090(2)	0.08456(9)	0.0132(5)	0.95(2)
Se1	8g	0.2862(2)	0.1226(2)	0.17593(9)	0.0193(3)	1
Se2	8g	0.1879(2)	0.4138(2)	0.0080(2)	0.0201(3)	1
Se3	4e	0.0000	0.0000	0.3214(2)	0.0306(6)	1
Cl1	2c	0.0000	0.5000	0.2500	0.041(2)	1
Cl2	2a	0.0000	0.0000	0.0000	0.036(2)	1

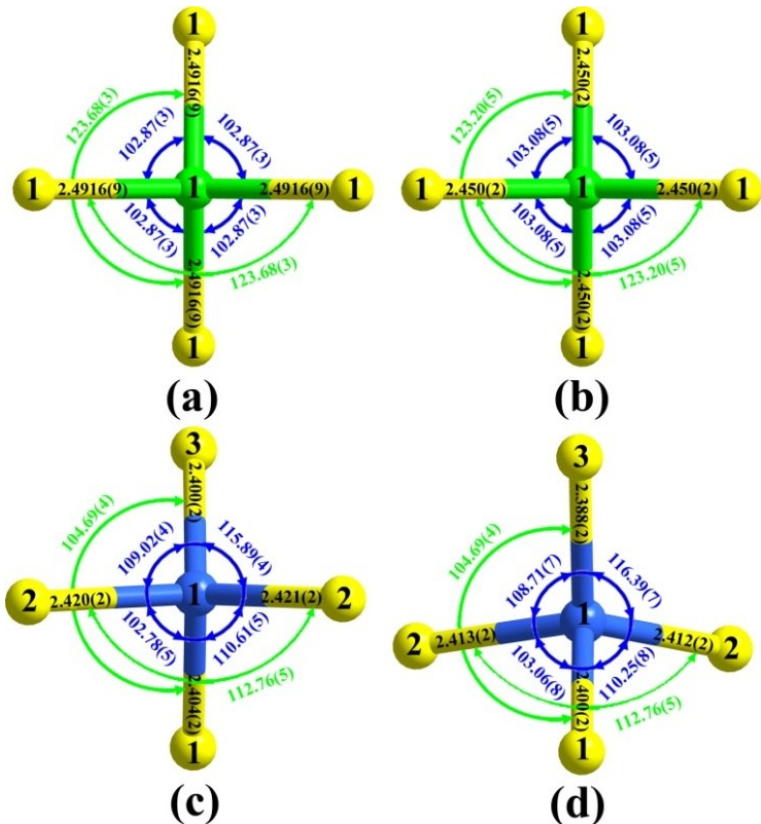


Figure S2. (a) and (b) The $\text{In}_y\text{Ga}_{4-y}\text{Se}_4$ T1 tetrahedron of $\text{Ba}_6\text{Cs}_2\text{In}_2\text{Ga}_8\text{Se}_{20}\text{Cl}_4$, **1** and $\text{Ba}_6\text{Cs}_2\text{InGa}_9\text{Se}_{20}\text{Cl}_4$, **2** with In/Ga–Se bond length (\AA) and Se–In/Ga–Se angle ($^\circ$) marked. (c) and (d) The $\text{In}_z\text{Ga}_{(1-z)}\text{Se}_4$ tetrahedron in T2 with In/Ga–Se bond length (\AA) and Se–In/Ga–Se angle ($^\circ$) marked.

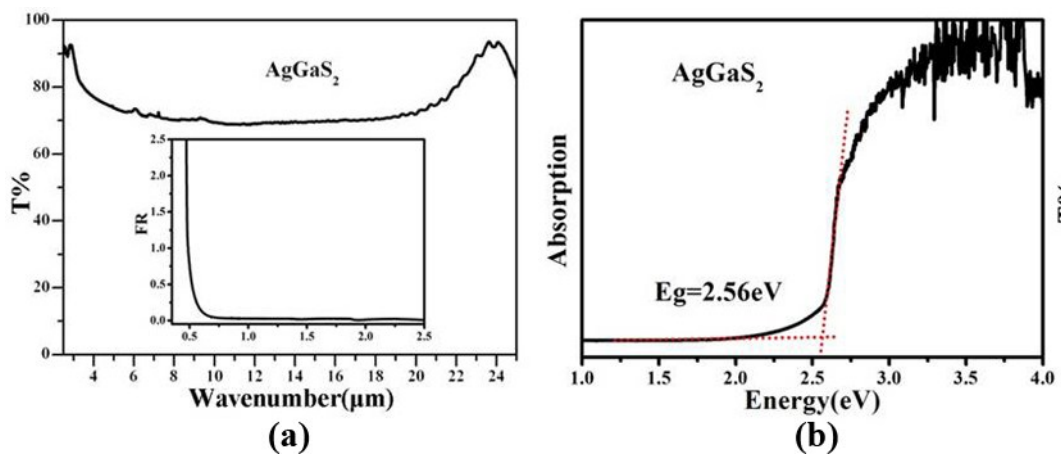


Figure S3. (a) Reflection spectra (inset) and FT-IR spectra, (b) Diffuse reflection spectra of AgGaS_2 .

Table S5. Selected bond lengths (Å) of $\text{Ba}_6\text{Cs}_2\text{In}_2\text{Ga}_8\text{Se}_{20}\text{Cl}_4$, **1** and $\text{Ba}_6\text{Cs}_2\text{InGa}_9\text{Se}_{20}\text{Cl}_4$, **2**.

$\text{Ba}_6\text{Cs}_2\text{In}_2\text{Ga}_8\text{Se}_{20}\text{Cl}_4$, 1		$\text{Ba}_6\text{Cs}_2\text{InGa}_9\text{Se}_{20}\text{Cl}_4$, 2	
Ba/Cs–Cl1	3.1214(6)	Ba/Cs–Cl1	3.1156(9)
Ba/Cs–Cl2	3.2039(6)	Ba/Cs–Cl2	3.199(2)
Ba/Cs–Se2	3.403(2)	Ba/Cs–Se2	3.394(2)
Ba/Cs–Se1	3.512(2)	Ba/Cs–Se1	3.500(2)
Ba/Cs–Se1	3.687(2)	Ba/Cs–Se1	3.672(2)
Ba/Cs–Se2	3.693(2)	Ba/Cs–Se2	3.682(2)
Ba/Cs–Se2	3.755(2)	Ba/Cs–Se2	3.757(2)
Ba/Cs–Se3	3.779(2)	Ba/Cs–Se3	3.760(2)
Ba/Cs–Se1	3.787(2)	Ba/Cs–Se1	3.827(2)
In1/Ga1–Se1×4	2.4916(9)	In1/Ga1–Se1×4	2.450(2)
In2/Ga2–Se3	2.400(2)	In2/Ga2–Se3	2.388(2)
In2/Ga2–Se1	2.404(2)	In2/Ga2–Se1	2.400(2)
In2/Ga2–Se2	2.420(2)	In2/Ga2–Se2	2.412(2)
In2/Ga2–Se2	2.421(2)	In2/Ga2–Se2	2.413(2)

Table S6. The calculated total energies of ideal single T1 or T2 substitution models of $\text{Ba}_6\text{Cs}_2\text{In}_2\text{Ga}_8\text{Se}_{20}\text{Cl}_4$, **1** (Model-1 (T1), Model-2 (T2)) and $\text{Ba}_6\text{Cs}_2\text{InGa}_9\text{Se}_{20}\text{Cl}_4$, **2** (Model-3 (T1), Model-4 (T2)).

Comp.	Model	Substitution occurs at	Total energy (eV)
$\text{Ba}_6\text{Cs}_2\text{In}_2\text{Ga}_8\text{Se}_{20}\text{Cl}_4$, 1	1	T1 site	-195.39
	2	T2 site	-195.04
$\text{Ba}_6\text{Cs}_2\text{InGa}_9\text{Se}_{20}\text{Cl}_4$, 2	3	T1 site	-195.97
	4	T2 site	-195.81

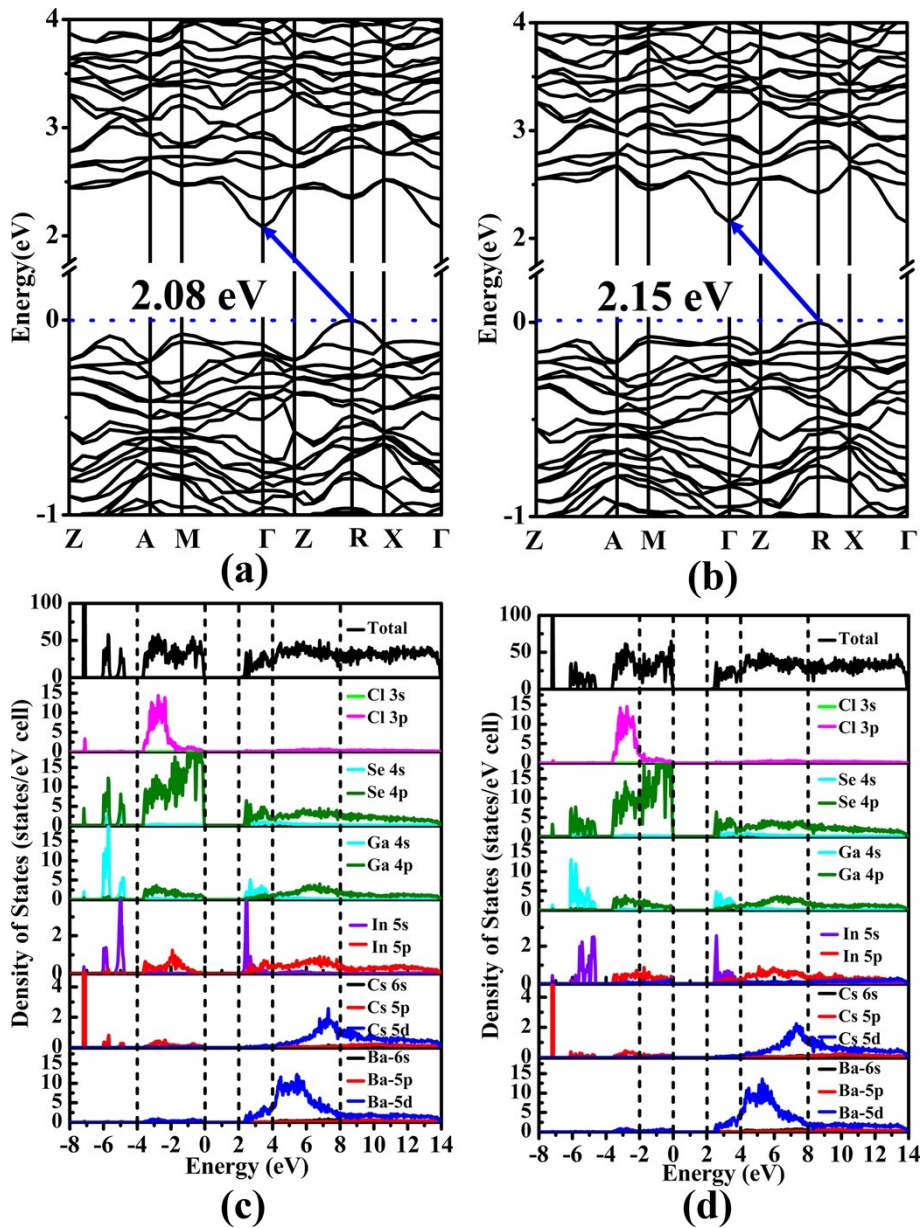


Figure S4. Band structures of $\text{Ba}_6\text{Cs}_2\text{In}_2\text{Ga}_8\text{Se}_{20}\text{Cl}_4$, **1** (a) Model 1 (T1) and (b) Model 2 (T2), total and partial densities of states of $\text{Ba}_6\text{Cs}_2\text{In}_2\text{Ga}_8\text{Se}_{20}\text{Cl}_4$, **1** (c) Model 1 (T1) and (d) Model 2 (T2).

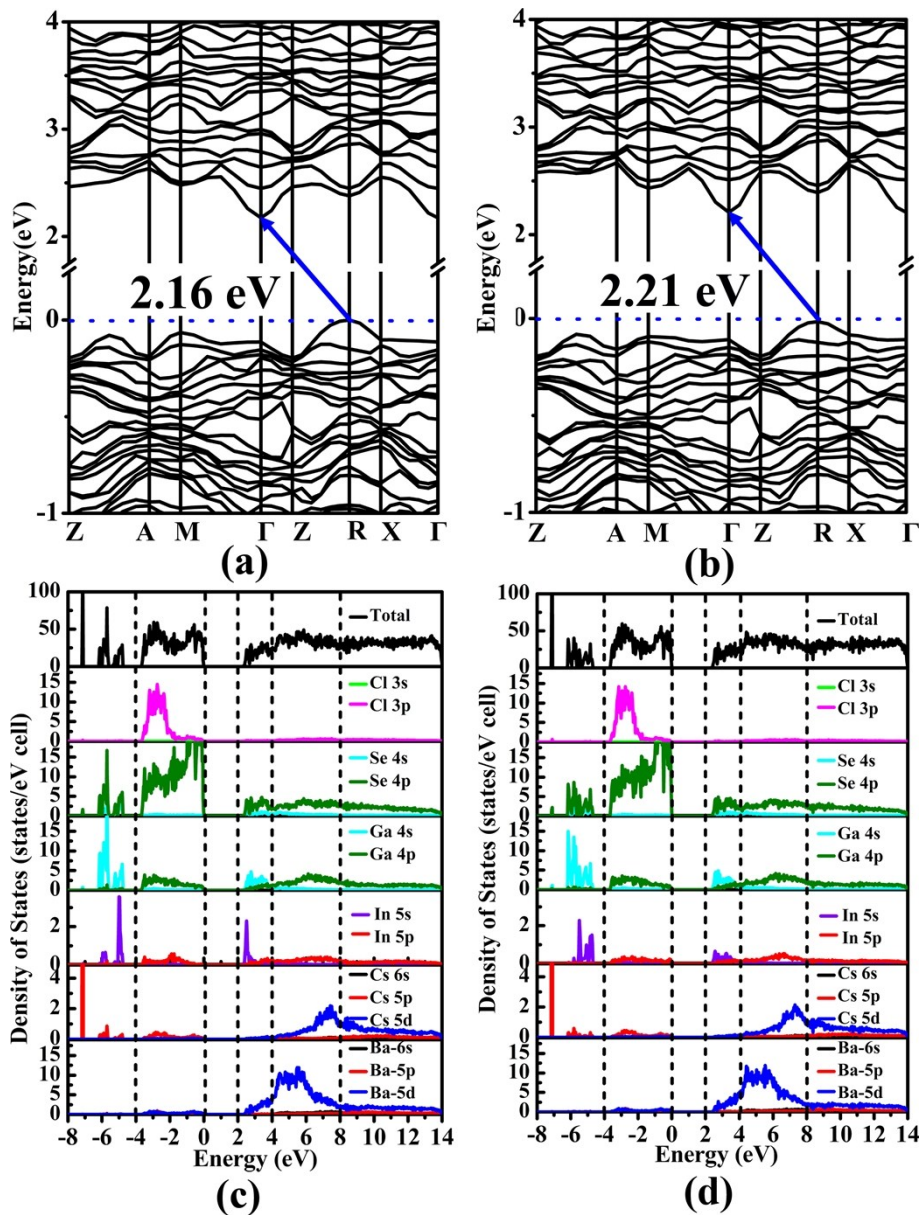


Figure S5. Band structures of $\text{Ba}_6\text{Cs}_2\text{InGa}_9\text{Se}_{20}\text{Cl}_4$, **2** (a) Model 3 (T1) and (b) Model 4 (T2), total and partial densities of states of $\text{Ba}_6\text{Cs}_2\text{InGa}_9\text{Se}_{20}\text{Cl}_4$, **2** (c) Model 3 (T1) and (d) Model 4 (T2).

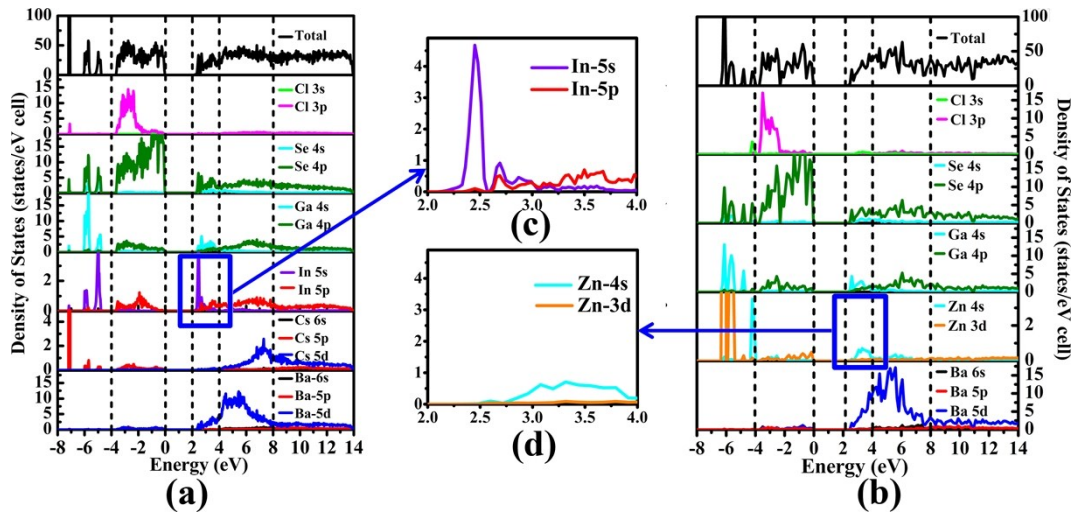


Figure S6. (a) Total and partial densities of states of $\text{Ba}_6\text{Cs}_2\text{In}_2\text{Ga}_8\text{Se}_{20}\text{Cl}_4$ (Model 1 (T1)), (b) Total and partial densities of states of $\text{Ba}_8\text{Zn}_2\text{Ga}_8\text{Se}_{20}\text{Cl}_4$, (c) Partial densities of states of In atom of $\text{Ba}_6\text{Cs}_2\text{In}_2\text{Ga}_8\text{Se}_{20}\text{Cl}_4$ (Model 1 (T1)) and (d) Partial densities of states of Zn atom of $\text{Ba}_8\text{Zn}_2\text{Ga}_8\text{Se}_{20}\text{Cl}_4$.